



Analysis of the Effect of Hull Vane[®] Lifting Force on Fast Vessel Resistance: Straight Hull Vane[®]

Nafiri Muhammad Kautsar¹, and I Ketut Suastika¹

¹ Department of Naval Architecture, Sepuluh Nopember Institut of Technology, Surabaya, 60111, Indonesia

Article Info

Article history:

Received July 17, 2023

Revised August 15, 2023

Accepted August 16, 2023

Keywords:

Hull Vane[®]

CFD

Lift Force

Resistance

ABSTRACT

In previous studies by Suastika, et al. (2020), the use of straight Hull Vane[®] increased the ship's resistance. Based on the hypothesis, this was caused by the lifting force from Hull Vane[®] being too large, so the ship experienced bow trim. To reduce bow trim, smaller Hull Vane[®] was made including Hull Vane[®] with Aspect Ratio (AR) = 8.5, AR = 22.9 and AR = 28.94 with speeds which were 11 knots (Fn = 0.34), 17 knots (Fn = 0.53), 20 knots (Fn = 0.62) and 26 knots (Fn = 0.8). From simulation results, it was found that the use of a straight Hull Vane[®] in every aspect ratio variation on the vessel was only effective at 11 knots speed which could reduce ship's resistance up to 17%. For speeds above 11 knots, an increase in aspect ratio can reduce resistance but resistance on ships with straight Hull Vane[®] was still greater than on ships without Hull Vane[®] because the lift force by Hull Vane[®] at the ship stern was still too large, so the bow of ship was more submerged than a ship without Hull Vane[®]. This caused the value of the Wetted Surface Area (WSA) and the value of hydrodynamic pressure more increased than ships without Hull Vane[®], so the value of ship's resistance also increased.

©2023 This work is licensed under Creative Commons

Attribution-NonCommercial-ShareAlike 4.0 International (CC BY-NC-SA 4.0).

Corresponding Author:

Nafiri Muhammad Kautsar

A Department of Naval Architecture, Sepuluh Nopember Institute of Technology, Surabaya, 60111, Indonesia

Email: nmkautsar@gmail.com

INTRODUCTION

There has been many studies that sought fuel energy efficiency in ships, one of which was by reducing drag on ships. Reducing drag on ships can be optimized by optimizing the hull-form design (Campana et al., 2018) and also using appendages such as stern wedges, stern

flaps, or Hull Vane[®] (Ferré et al., 2019).

To optimize the use of Hull Vane[®], Sepuluh Nopember Institute of Technology also takes part in research on the development of Hull Vane[®]. Previously, research was carried out regarding the installation of the Hull Vane[®] on the transom of the ORELA crew boat by

Suastika, et al. (2020). This study aimed to determine the effect of the V-shaped and straight-shaped Hull Vane[®] on the ship's resistance as shown in Figure 1.

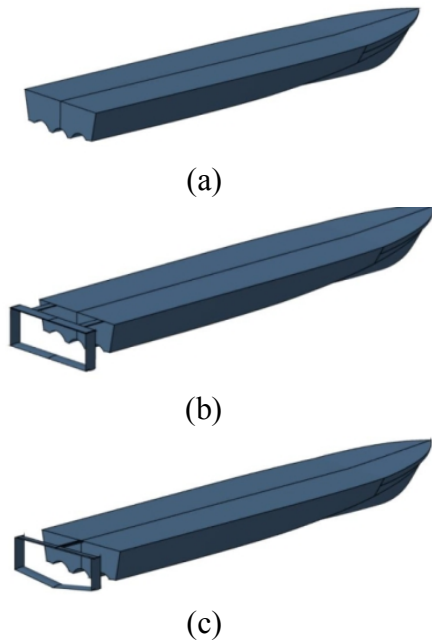


Figure 1. Hull Vane[®] geometry on crew boat: (a) without vanes, (b) with straight vanes, (c) with V vanes (Suastika et al., 2020)

However, the results obtained were considered unsatisfactory because at Froude Number (F_n) > 0.6 or speeds > 20 knots, the presence of Hull Vane[®] resulted increase in the total resistance of the ship for both ships with straight Hull Vane[®] and ships with Hull Vane[®] V. This occurred due to the force the lift force on the Hull Vane[®] was too large, so that the ship's position became slightly bent at the bow (Suastika et al., 2020).

Because of those problems, this research is aimed to analyze the effect of lift force generated by straight-shaped Hull Vane[®] to the resistance of fast vessels. In this case, fast vessel which used as the object of research was the ORELA crew boat. The analysis in this study is to compare the total resistance on the ship when experiencing a lift force from the Hull Vane[®] with variations in the aspect ratio.

LITERATURE REVIEW

Working Principle of Hull Vane[®]

The working principle of the Hull Vane[®] provides additional thrust on the x-axis and also provides lift on the z-axis (Uithof et al., 2014). Technically, there are 4 effects produced by using Hull Vane[®], including:

1. Thrust Force

According to Uithof, et al. (2014), foil creates a lift force vector L_{HV} with a vector perpendicular to the direction of the flow of fluid and a drag force vector D_{HV} in the same direction as the direction of fluid flow as shown in Figure 2. The resulting force generated from the F_{HV} vector can be composed as x and z components as in Equation (1).

$$L_{HV} + D_{HV} = F_{HV} = F_{x,HV} + F_{z,HV} \quad (1)$$

L_{HV} = lift force Hull Vane[®] (N);
 D_{HV} = drag force Hull Vane[®] (N); F_{HV} = resultant force Hull Vane[®] (N); $F_{x,HV}$ = force Hull Vane[®] on x-axis (N); $F_{z,HV}$ = force Hull Vane[®] on z-axis (N).

If the effect of the x component on the lift vector is greater than the x component on the drag vector. Then it is possible to produce the resultant force on the x component. The magnitudes of L_{HV} and D_{HV} can be estimated by Equation (2) and Equation (3). It should also be noted that the magnitudes of Coefficient of Lift (C_L) and Coefficient of Drag (C_D) are not only depend on the shape of the foil used but also depend on the vicinity of the free surface.

$$= - \quad (2)$$

$$= - \quad (3)$$

ρ = density (kg/m³); v = velocity (m/s);
 A = foil area (m²).

Then, if θ is defined as the trim angle, the

thrust generated by the Hull Vane[®] can be described by the Equation (4).

$$F_{HV} = \sin(\alpha + \beta + \theta) L_{HV} - \cos(\alpha + \beta + \theta) D_{HV} \quad (4)$$

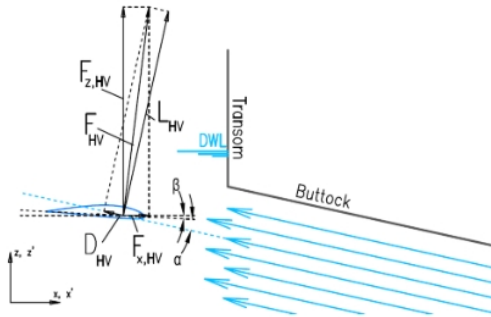


Figure 2. Working principle of Hull Vane[®] (Uithof et al., 2014)

2. Trim Correction

When the ship operates at a transition speed, the ship will experience dynamic trim where each speed will have a different trim angle. The trim angle on a moving ship is very different from that on a stationary ship (Ferré et al., 2019). The force generated by the Hull Vane[®] in the z direction vector greatly affects the balance of the ship by reducing dynamic trim and keeping the ship in an even keel condition at higher speeds. In addition, by reducing the trim, this force can also affect the angle of attack of the water flow on the Hull Vane[®] (Uithof et al., 2014).

3. Reducing Waves

With the use of Hull Vane[®], it is proven to be able to reduce ship waves. The flow along the Hull Vane[®] creates a low pressure area on the top surface of the Hull Vane[®] thereby causing beneficial interference to the waves generated by the ship's transoms, significantly reducing the wave profile (Uithof et al., 2014).

4. Reduction of Wave Motion

According to Ferré et al. (2019) that the addition of Hull Vane[®] to ships can reduce ship resistance due to ship movements due to waves

such as pitching, heaving, rolling and yawing by 10% to 30%. In addition, when the ship is pitching, the Hull Vane[®] will generate additional thrust force which is called the pumping effect.

Effect of Hull Vane[®] Location

Over the last few years, there have been many studies focused on determining the optimal position of the Hull Vane[®] relative to the ship's hull. When the Hull Vane[®] is installed too close to the hull, it is not profitable. This position is likely to be in the boundary layer as well as it reduced lift generated in results. In addition, the low pressure area at the top of the Hull Vane[®] will bounce off the hull so that it can increase the pressure resistance especially if the Hull Vane[®] is fully submerged. To avoid this, the Hull Vane[®] installation position needs to be pushed back a little but with the risk of reducing the thrust generated by the Hull Vane[®] (Uithof et al., 2014).

Riyadi & Suastika (2020) also conducted another study by testing the position of the Hull Vane[®] with variations in the position of the leading edge foil right behind the transom, the position of the leading edge foil 1 chord behind the transom, and the position of the leading edge foil 2 chords behind the transom. Tests were conducted experimentally in towing tanks which were then verified numerically via Computational Fluid Dynamics (CFD) with multiphase free surface analysis. The results obtained were that the Hull Vane[®] installed 2 cords behind the transom gave the best drag reduction results of 11.14% experimental test results at $Fn = 0.74$ and a reduction of 15.22% at $Fn = 0.7$. Reducing total resistance greatly affects the value of the Froude Number so that reducing barriers could only occur in a certain range of Froude Numbers (Riyadi & Suastika, 2020).

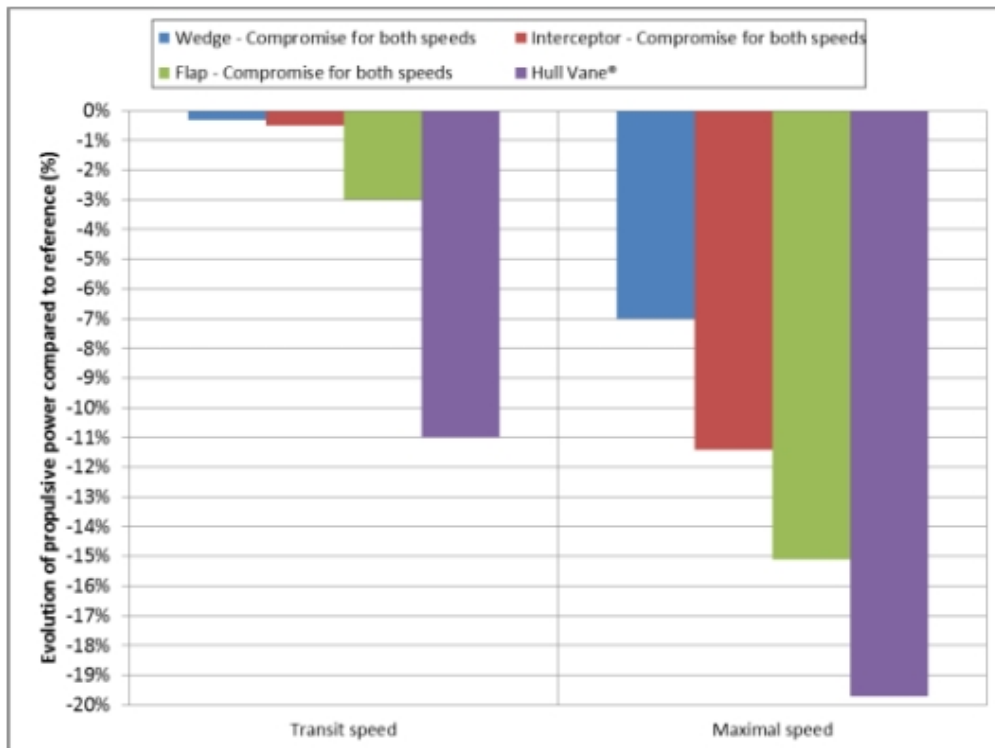


Figure 3. Resistance comparison between the use of Hull Vane[®], stern wedge, stern flap and interceptors (Ferré et al., 2019)

Comparison of Resistance Reduction with Various Appendages Forms

The use of Hull Vane[®] is more effective than the addition of other forms of appendages on ships such as stern flaps, stern wedges and interceptors. In Figure 3, it can be seen that the reduction in resistance by Hull Vane[®] is better than the others at transit speed and maximum speed (Ferré et al., 2019).

Lift and Drag

Any object that moves in the fluid flow will experience forces due to the interaction between the fluid flow and the surface of the object. Technically, the components of the force are lift force and drag force. In aerodynamics, lift is the force that directly opposes the weight of the aircraft and keeps the aircraft in the air. Lift is generated in every part of the plane, but most of it comes from the lift on the plane, which is then known as the airfoil. Lift occurs when a moving gas stream is rotated due to the influence

of interactions with solid objects. This is due to the difference in velocity between the solid object and the fluid which will then produce a force component in the form of a lift force that works perpendicular to the movement and a drag force that works in the opposite direction to the object's movement as shown in Figure 4 (Hall, 2022a).

However, there are several erroneous theories regarding the airfoil interaction that generates the lift force. The theory in question is the "Longer Path" theory or the "Equal Transit Time" theory. The theory states that airfoils are formed with the top longer than the bottom. So for the same fluid molecules, the molecules passing through the top of the airfoil must move faster than the molecules moving below the airfoil to meet at the trailing edge. This theory was declared wrong after conducting experimental tests which stated that the same molecules would not meet at the trailing edge because the movement of molecules at the top of

the airfoil moved faster than predicted so that the molecules reached the trailing edge first compared to molecules moving at the bottom of the airfoil (Hall, 2022b).

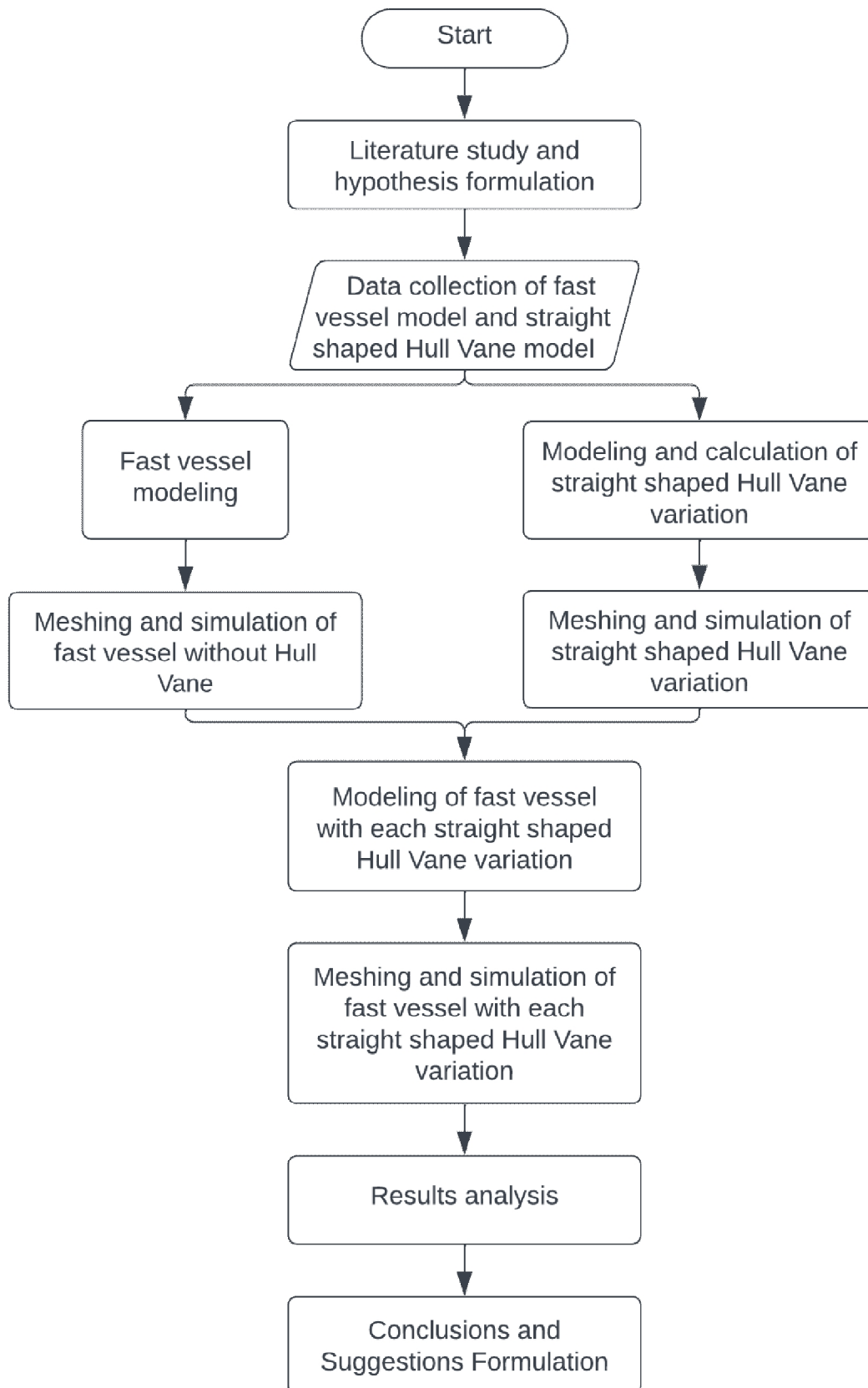


Figure 5. Research methodology flowchart

This also causes the lift force to be able to support the weight of the object through the airfoil because of the very large difference between the magnitude of the fluid velocity at the top and bottom of the airfoil. This speed difference results in a large pressure difference where the pressure at the bottom of the airfoil is greater than at the top. This theory is called Bernoulli's principle (Bernoulli's law) which states that an increase in speed must accompany every reduction in pressure.

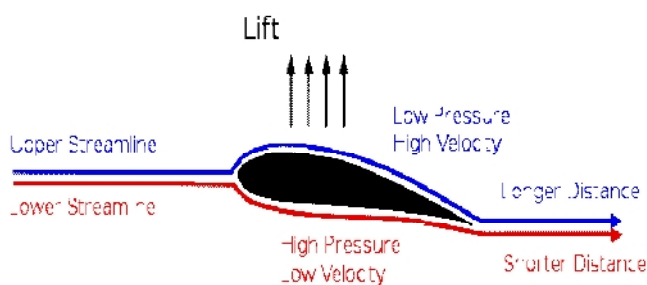


Figure 4. Airfoil working principle (Hall, 2022b)

In addition, the angle of attack is also a factor in increasing the lift force. The greater the angle of attack, the lift force will increase at several critical angles. This is because the fluid is deflected through a larger angle so that the vertical component of the fluid flow velocity increases (Hall, 2022c).

The aerodynamic force acting on the foil has the following general Equation (5).

$$F = C_f \cdot \rho \cdot V^2 \cdot A \quad (5)$$

F = force (N); A = surface area of force (m²); C_f = coefficient of force.

NACA Airfoil Series

The type of foil used in this study is NACA 6-Series. This series was developed with a more complicated shape and using a more theoretical method, compared to previous generations which were developed with a geometric method. The theoretical method used is to determine the

desired pressure distribution on the foil, then proceed with determining the appropriate foil geometry shape. This aims to maximize the area of laminar fluid flow on the foil so the resistance is smaller than the previous NACA series (Selvaraj et al., 2017).

For the specific shape, this study uses the NACA 64(1)-212 foil type, due to the good performance that this airfoil provides in subsonic flight and its relatively high critical Mach number (Ghidoni, 2017). In addition, this airfoil has been used as the object of research several times in previous studies.

The variation of foil size on Hull Vane[®] used in this study was adjusted to the Hull Vane[®] aspect ratio that had been previously determined by reducing the percentage of Force Lift (%F_{Lift}) to C_L at AR = 8.5, which was then determined within the delimitation of problems, including AR = 8.5, AR = 22.9 and AR = 28.94. Then from the lift force, the amount of cord used is measured with a fixed span of 6.8 m. So that we get a variation of the shape of the foil on the Hull Vane[®].

METHOD

Research method consists nine primary steps with literature study and hypothesis formulation combined. To simplify visualization of research method, the flowchart of research method can be seen in Figure 5.

Literature Study and Hypothesis Formulation

This stage was the fundamental stage because the writer was required to look for various sources of information and related references regarding the related topic so that the writer completely understood the comprehension of the related topic. The intended sources came from books, scientific journals, expert opinions, and even research that had been done before.

Then, after gathering enough references, we needed to determine a provisional hypothesis before simulating it so that the research conducted could be more directed and had a purpose.

Data Collection of Fast Vessel Model and Hull Vane® Foil

The requirement of data was the ship's lines plan so that the shape of the hull can be known. In addition, data regarding the type of foil for Hull Vane® and struts was also needed. In this case, the Hull Vane® used the NACA 64(1)212 series, and the struts used the NACA 0010 series. Other data that may be needed was data from previous studies regarding the use of Hull Vane® on fast vessels, so that it could be a reference as well as comparative data for this study.

The 3D model of a fast vessel was made with the Maxsurf Modeler software which made based on the ship's lines plan. Furthermore, the main dimensions of the 3D ship model that had been designed needed to be compared with the original ship. It was intended for checking the validity of the model used.

Meshing Process and Simulation of Fast Vessels without Hull Vane®

This stage was one of the key stages in the process of CFD software because it determined the quality of the simulation results. Meshing was the process of discretizing the continuous fluid domain into a discrete computational domain so that it could be solved with fluid flow equations.

Then after the meshing process was done, a simulation process was carried out in CFD with the setup that was done before. In this case, the software used was FINE/Marine software. Numerical model tests were carried out with each predetermined speed variation, namely at speeds of 11, 14, 17, 20, 23, and 26 knots.

Modeling and Calculation of Straight Shaped Hull Vane®

Hull Vane® 3D modeling was made by using AutoCAD software. Model variations made based on the previously determined Hull Vane® aspect ratio including AR = 8.5, AR = 22.9 and AR = 28.94.

Crew Boat Modeling with Each Hull Vane® Model Straight Shaped

After modeling the ORELA Crew Boat and the straight-shaped Hull Vane®, it was also necessary to do 3D modeling of the ORELA Crew Boat which had been installed with straight-shaped Hull Vane® model with a position at 2 chord lengths behind the transom. This process of modeling was made using AutoCAD and Rhinoceros software.

Meshing Process and Fast Vessel Simulation without Hull Vane® and each Hull Vane® Variation

This process was the same as before, but it used the ship model that had been installed with the Hull Vane® variation. Therefore, the number of elements in the meshing was made more than the meshing on the ship without Hull Vane®. The reason was the small shape of the Hull Vane® pieces required more detailed and accurate meshing. Then the simulation was carried out with CFD analysis with fewer speed variations from the ship without Hull Vane® simulations at speeds of 11, 17, 20, and 26 knots.

Data Analysis and Discussion

At this stage, the analysis results were obtained from running CFD simulations on each model variation. Then all the results obtained in each model variation are compared and explained in detail through the discussion.

Conclusions and Suggestions

This stage was the conclusion of the analysis of the results that have been obtained previously. Then the evaluation as well as criticism and suggestions during the research will be explained at this stage as well.

RESULTS AND DISCUSSION

Modeling 3D Ship Without Hull Vane[®]

Table 1. Deviation of hydrostatic data between the 3D ship model and the actual ship

No	Item	Data		Unit	Deviation
		Ship	3D model		
1	L _{OA} (Length Over All)	31	31	m	0.00%
2	L _{WL} (Length Waterline)	28.4	28.408	m	0.03%
3	B (Breadth)	6.9	6.9	m	0.00%
4	T (Draft)	1.4	1.4	m	0.00%
5	Displacement	104.33	104.9	ton	0.55%
6	WSA (Wetted Surface Area)	177.13	177.091	m ²	-0.02%
7	C _B (Block Coefficient)	0.409	0.415		1.47%
8	C _M (Midship Coefficient)	0.47	0.478		1.70%
9	C _{WP} (Water-plane Area Coefficient)	0.83	0.825		-0.60%
10	L _{CB} (Longitudinal Centre of Bouyancy)	11.79	11.766	m	-0.20%
11	L _{CF} (Longitudinal Centre of Floatation)	11.44	11.465	m	0.22%

The 3D model ship design was made based on the original crew boat that had been built so that the 3D model design must be similar to the original ship with a maximum deviation limit of around 2%. The lines plan on the 3D model can be seen in Figure 6, while the hydrostatic data comparison between the 3D ship model and the actual ship can be seen in Table 1.

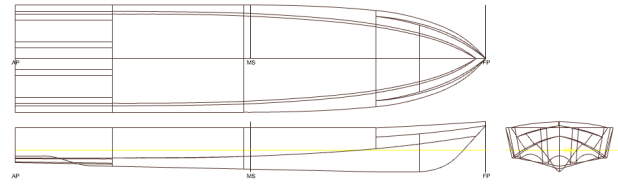


Figure 6. Lines plan 3D ship model

Based on Table 1, the largest deviation at C_M was 1.7%. It meant that all of the data did not exceed the tolerance limit of 2% so that the ship model design was considered valid according to the actual ship.

Modeling of Straight Hull Vane[®]

The foil test in this study was not simulated but it used the finite-span theory because the variations of foil used were still on the same type of foil, namely NACA 64(1)-212 (White, 2011). The difference in variations is based only on the size of the geometry, namely with a fixed span size of 6.8 m. The calculation of foil was calculated by comparing the aspect ratio of the foil geometry. Then, for a certain C_L, the horizontal shift in α due to AR changes could be calculated by Equation (6).

$$\Delta\alpha = \frac{C_L}{AR} \quad (6)$$

To validate the calculation results, it was necessary to do a comparison with the foil simulation that had been done before. The comparison graph of the coefficient of lift (C_L) in the previous simulation and calculations using the finite-span theory could be seen in Figure 7. From the graph, it could be seen that the graph values coincided with each other so it could be said that the calculations carried out were valid.

Furthermore, the calculation of Hull Vane[®] characteristic data for each AR was carried out with C_L values at $\alpha = 2^\circ$. Then, the lift force calculation was carried out with Equation (6) according to the AR that had been determined

from the Hull Vane[®] variation used. To determine the value of C_L at $\alpha = 2^\circ$ in each variation, it was necessary to do calculations according to the finite span theory as the Equation (7) to obtain a horizontal shift in α due to AR changes.

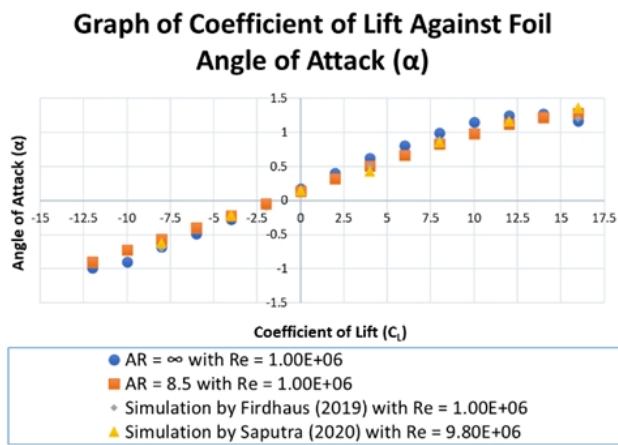


Figure 7. Comparison of coefficient of lift in previous simulations and finite-span calculations

Then it was also necessary to calculate the Hull Vane[®] lift force for each AR. The calculation was done with the following Equation (7).

$$0.5 \cdot \dots \cdot \dots \quad (7)$$

= lift force (N); b = span length (m);
 c = chord length (m).

Calculations were made with a maximum speed of 26 knots. After doing the calculations, the lift force values generated by Hull Vane[®] are obtained, among others, at AR = 8.5 it produced a F_{Lift} of 161,745.5 N, at AR = 22.9 it produced a F_{Lift} of 67,780.3 N, and at AR = 28.94 it produced a F_{Lift} of 54,617.5 N.

Modeling 3D Ship with Hull Vane[®]

After checking the 3D deviation of the ship model with the original ship, the modeling process could proceed to the next stage which was modeling ships that have been installed with each Hull Vane[®] variation. The type of Hull

Vane[®] and struts used were determined in the delimitation of problems which were NACA 64(1)-212 for Hull Vane[®] and NACA 0010 for struts. The size variation of Hull Vane[®] used was also determined on the delimitation of problems including Hull Vane[®] with size AR = 8.5, size AR = 22.9 and size AR = 28.94 which were installed at 2 chord lengths behind the transom as shown in Figure 8.

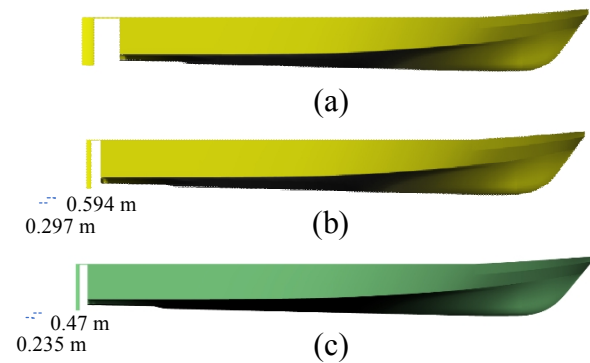


Figure 8. Side view of the ship model with Hull Vane[®] in each variation; (a) with AR = 8.5, (b) with AR = 22.9 and (c) with AR = 28.94

Ship Simulation Results Without Hull Vane[®]

The simulation was carried out with Fine Marine Numeca software and used the following domain sizes:

1. 1.5 times L_{OA} to the bottom of the ship;
2. 1 time L_{OA} towards the ship;
3. 1.5 times L_{OA} towards the front of the ship;
4. 2 times L_{OA} to the side of the ship; and
5. 3 times L_{OA} towards the back of the ship.

Then the meshing process was carried out with the result as shown in Figure 9 and the simulation process was continued, so that the resistance value for each speed variation was obtained as shown in the following Table 2.

The resistance value that has been obtained from the simulation results needed to be validated. Validation was carried out by comparing the resistance values from the simulation results with experimental results, Savitsky simulation results on Maxsurf resistance

and CFD simulation results in previous studies. The following graph was the resistance values compares as shown in Figure 10.

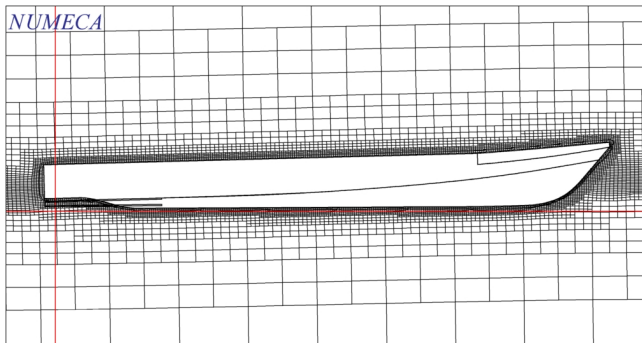


Figure 9. Ship meshing without Hull Vane[®]

Table 2. Resistance values in ship simulations without Hull Vane[®]

CFD Simulation	Number of elements	Resistance (N)
11	2,534,815	22,956.04
14	2,553,614	39,715.40
17	2,976,132	55,086.22
20	2,587,146	72,044.94
23	2,732,966	80,312.12
26	2,669,977	94,337.64

COMPARISON OF RESISTANCE FROM SHIP SIMULATION WITHOUT FOIL

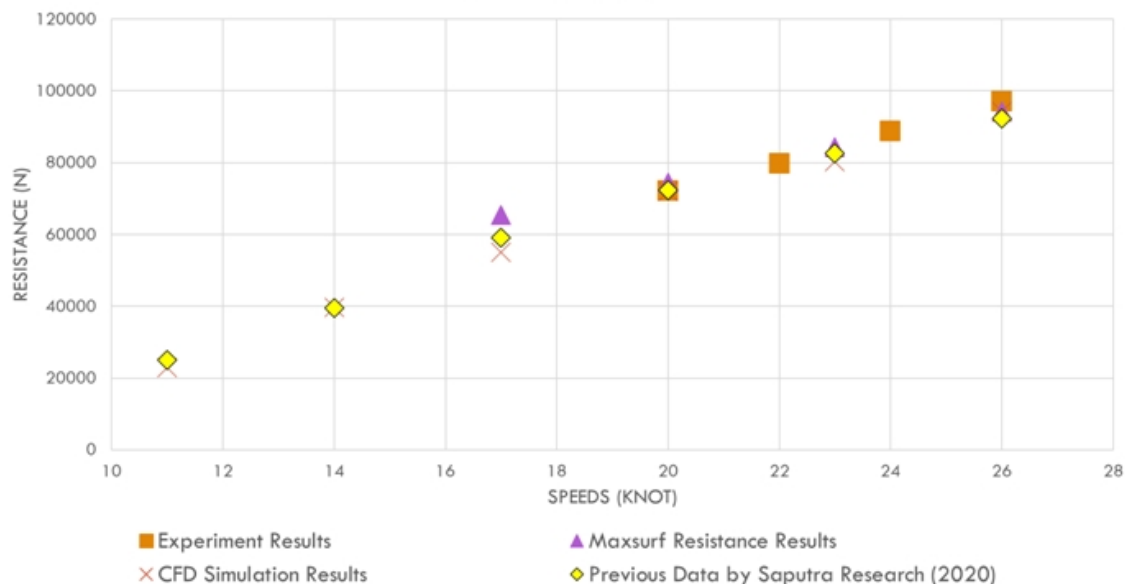


Figure 5. Graph of resistance comparison of ship simulation results without Hull Vane

Ship Simulation Results with Straight Hull Vane[®]

The CFD simulation was carried out using the Fine Marine Numeca software. The simulation results for each Hull Vane[®] variation could be seen in Figure 11.

Based on the data obtained, it could be concluded that ships with straight Hull Vanes[®] only reduced ship resistance at speed 11 knots ($F_n = 0.34$) but at higher speeds, ($F_n > 0.34$) there was an increase in ship resistance at the foil variation $AR = 8.5$, $AR = 22.9$ and $AR = 28.94$.

The increase of resistance when using Hull Vane[®] was quite significant, if it was compared to the value of resistance on the ship without Hull Vane[®]. Deviation data could be seen in Table 3.

This increase of resistance was caused by various factors. However, the biggest factor was the existence of the Hull Vane[®] which provided a lift force on the ship, thus creating a difference in the Wetted Surface Area (WSA). Ships using straight Hull Vane[®] in each variation had a larger WSA than ships without Hull Vane[®]. This was

caused by the existence of the Hull Vane[®] itself which increased immersed area as well as the influence of the lift force from straight Hull

Vane[®] which was too large, so that the ship became bow trim.

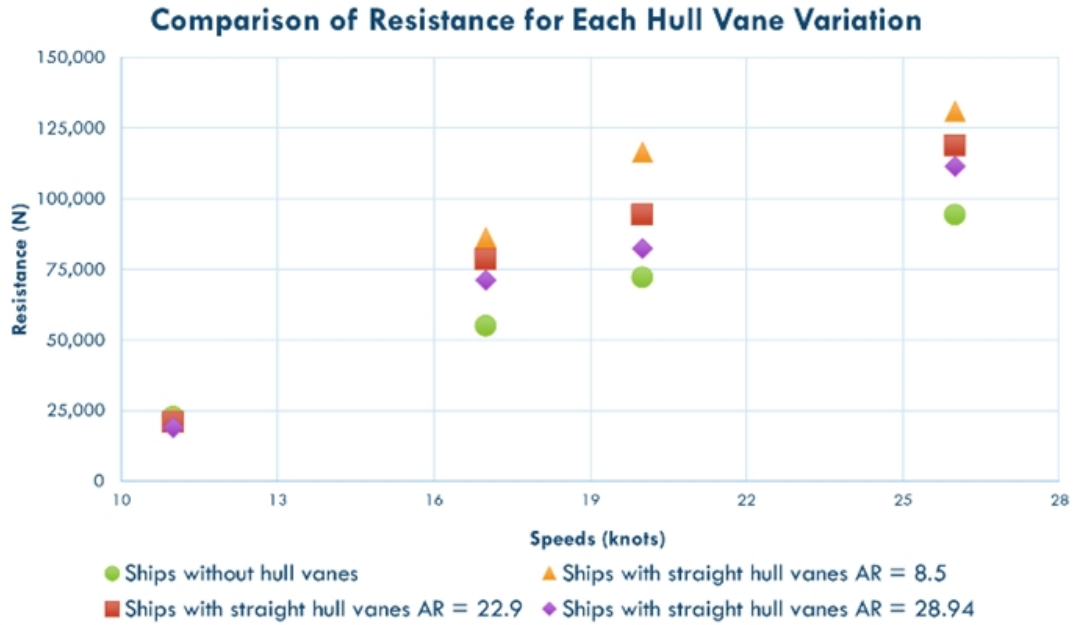


Figure 6. Comparison of ship resistance at each Hull Vane[®] aspect ratio

Table 3. Comparison of resistance deviation

Deviation of resistance values between ships without Hull Vane [®] and ships with Hull Vane [®] in each variation			
	at AR = 8.5	at AR = 22.9	at AR = 28.94
	-2%	-9%	-17%
	57%	43%	29%
	62%	31%	14%
	39%	26%	18%

1. Comparison of Trim Angle Values

The trim angle on the ship could indicate the pitch movement of the ship. If the ship's angle was positive, then the ship experienced a bow trim whereas if the ship's angle was negative, then the ship experienced a stern trim or a planning ship condition. It could be seen from the data in Table 4, that ships without Hull Vane[®] generally experienced planning. Then the

ship with the Hull Vane[®] AR = 8.5 variation had the greatest trim angle value so that the bow of the ship was more bowed.

Table 4. Comparison of the ship trim angle values for each variation

Variations in the Use of Hull Vanes [®]	Speed (knots)			
	11	17	20	26
Ships without Hull Vane [®]	0.442	-0.861	-1.343	-1.497
Ships with straight Hull Vane [®] AR=8.5	1.553	0.083	-0.338	0.373
Ships with straight Hull Vane [®] AR=22.9	1.187	-0.029	-0.482	-0.196
Ships with straight Hull Vane [®] AR=28.94	1.039	-0.313	-0.490	-0.248

This also caused the resistance value in the AR = 8.5 variation to be the largest on average

compared to other variations. To simplify data visualization, a comparison of the trim angles in

each variety of foil sizes could be seen in Figure 12.

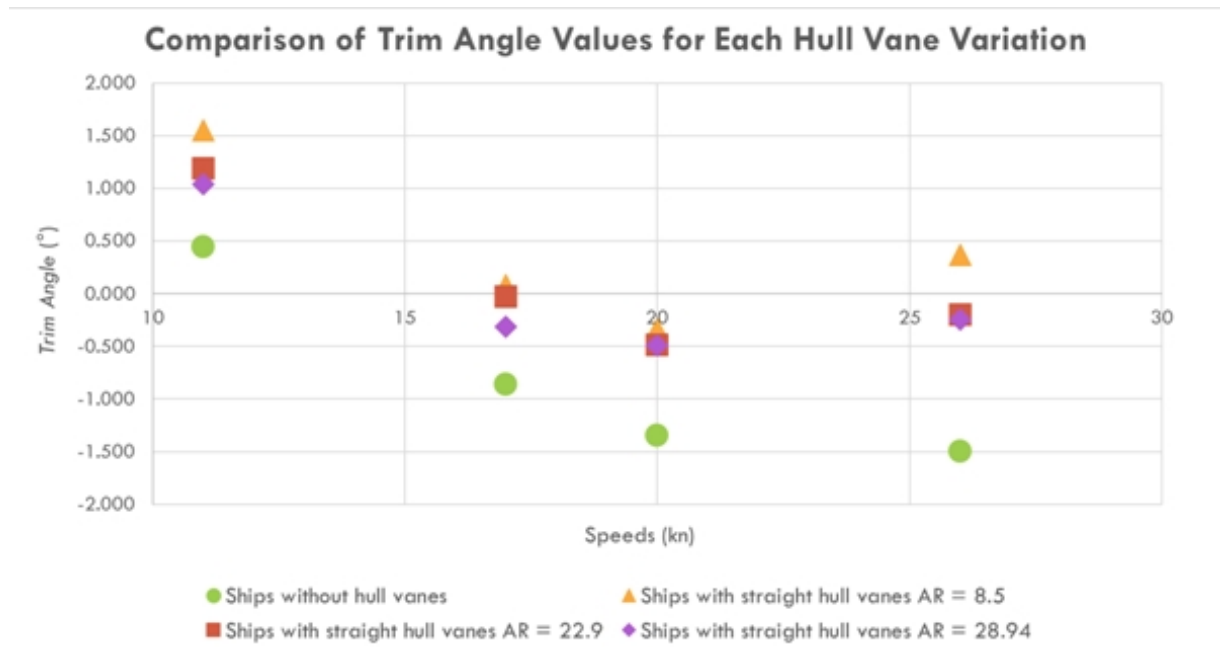


Figure 7. Comparison of trim angle values for each aspect ratio

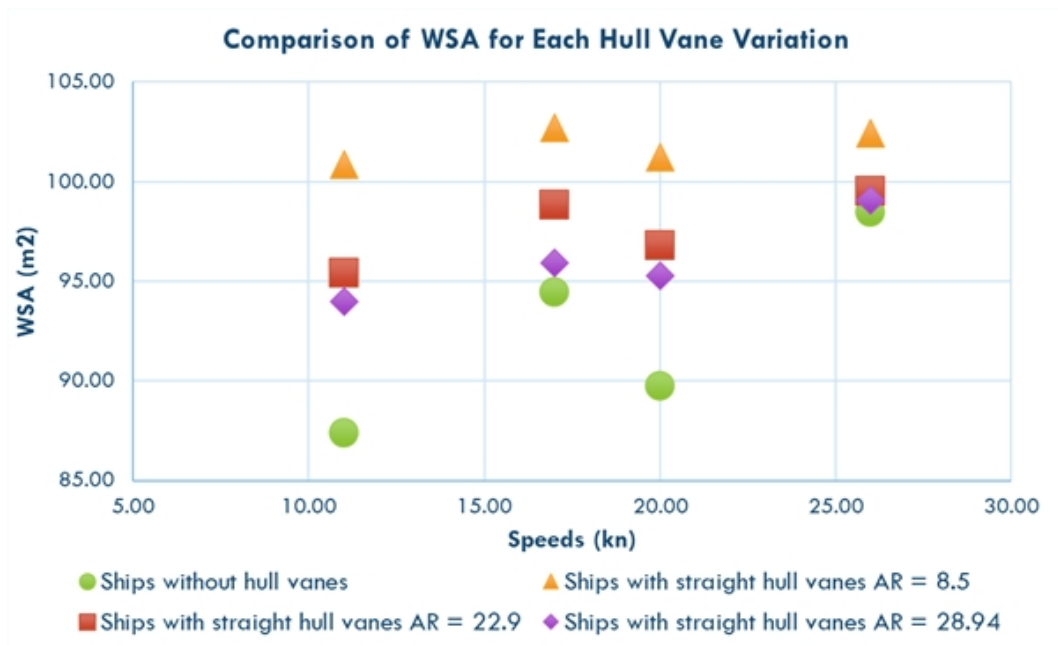


Figure 8. Comparison of WSA values for each aspect ratio

2. Comparison of WSA Values

The WSA value on the ship was very impactful for the value of the ship's resistance. The greater the WSA value of the ship, the greater area of the ship that was submerged which directly influenced the increase of ship

resistance. The WSA value for each variation can be seen in Figure 13.

3. Comparison of Hydrodynamic Pressure Values

Beside the WSA value that affects the resistance value, the hydrodynamic pressure

value also affected the resistance value because the pressure from water could increase the resistance value on the ship. To observe more detail, it was necessary to select a specific surface area, then the selected area would be compared in each variation. The specified

surface was located on the ship's bottom plate because all parts of this surface were submerged in water, so that the distribution of pressure on the surface could be seen in more detail. Hydrodynamic pressure values for each variation could be seen in Figure 14.

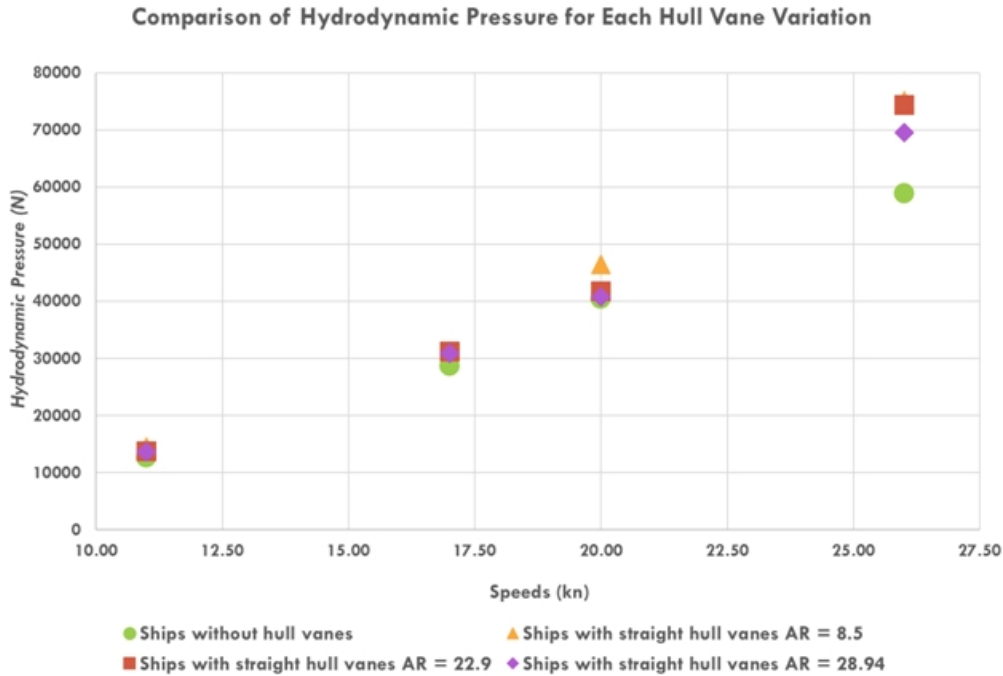


Figure 9. Comparison of hydrodynamic pressure values for each aspect ratio

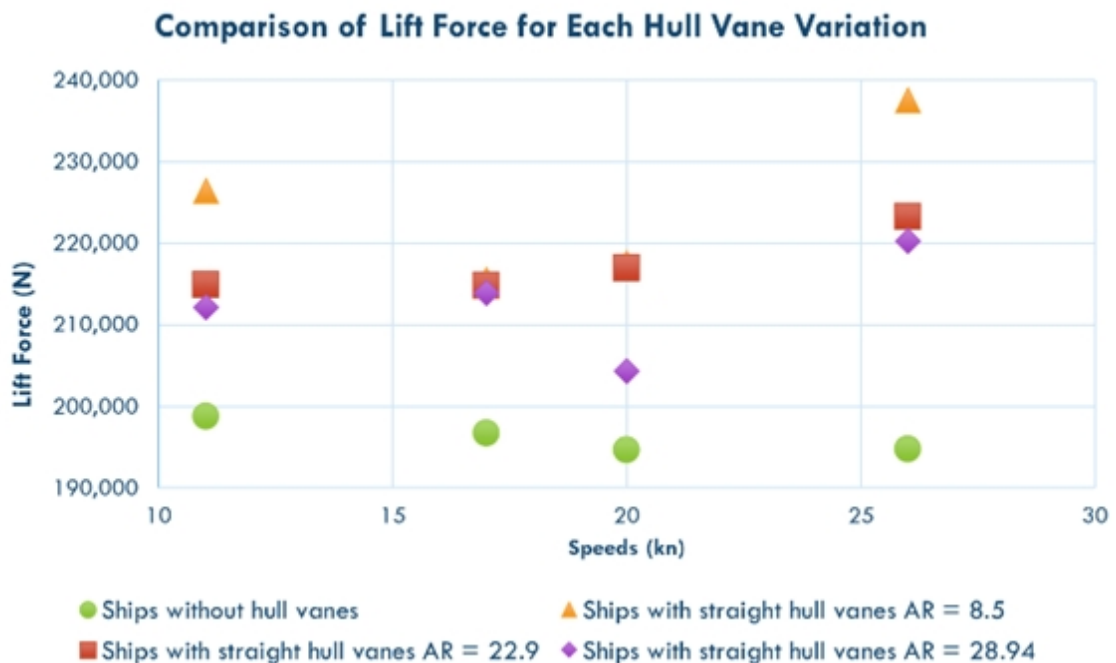


Figure 10. Comparison of lift force for each aspect ratio

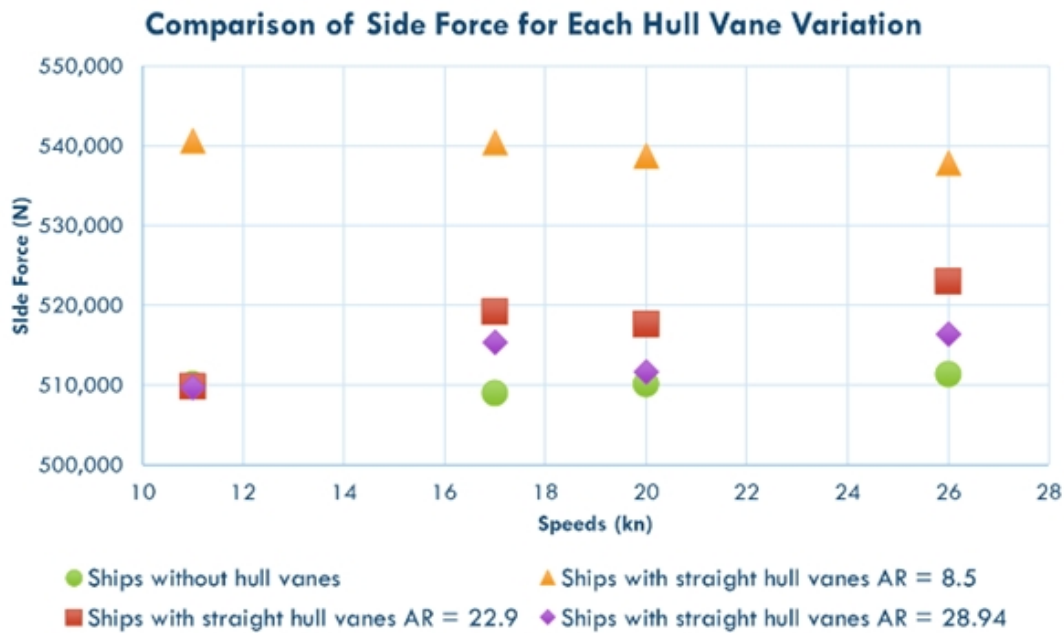


Figure 11. Side force comparison for each aspect ratio

4. Comparison of Lift Force and Side Force for Each Hull Vane[®] Aspect Ratio

The purpose of estimating the lift force and side force values was to show the effect of the Hull Vane[®] size aspect ratio on the total lift force and side force values of the ship. The simulation results showed that there were 3 aspect ratios, including ships with Hull Vane[®] size AR = 8.5, ships with Hull Vane[®] size AR = 22.9 and ships with Hull Vane[®] size AR = 28.94.

Based on the data obtained as shown in Figure 15, the trend on the graph was consistent for each variation which the total lift force value was the smallest on a ship without a Hull Vane[®]. Then, with the existence of the Hull Vane[®], the total lift force value inclined according to larger size of the Hull Vane[®]. This could be seen in the graph of the lift force values on ships with Hull Vane[®] AR = 8.5 having the greatest value. Furthermore, on the second aspect ratio which is 22.9 and the third aspect ratio which is 28.94, the lift force value consistently declined at each speed. This proved that the presence of Hull Vane[®] could increase the lift force value. If the

Hull Vane[®] chord size is larger, then the lift force value would be greater too.

Furthermore, for side forces, it were not different from the trend in lift forces which the presence of Hull Vane[®] also added side forces. However, there was a slight difference at a speed of 11 knots, the side force values on ships with Hull Vane[®] AR = 22.9 and AR = 28.94 were smaller than the side force values on ships without Hull Vane[®]. Then it could also be seen in Figure 16, the graph that a ship with a Hull Vane[®] AR = 8.5 had the greatest side force value compared to the aspect ratio of other Hull Vane[®] at each speed. Furthermore, in the second aspect ratio with AR=22.9 and the third aspect ratio with AR=28.94, the side force value consistently decreased compared to the Hull Vane[®] side force value AR = 8.5 at each speed. This proved that the larger size of Hull Vane[®] chord, then greater the side force tends to be.

CONCLUSION

Through the simulation results that had been carried out, it can be concluded that the use

of a straight Hull Vane[®] on a ship was only effective for reducing resistance at $F_n = 0.34$ or a speed of 11 knots. Whereas at $F_n > 0.34$ or speeds greater than 11 knots on the ship, it proved ineffective because its presence increased the total resistance by up to 62% compared to the total resistance on the ship without Hull Vane[®]. The addition of Hull Vane[®] resistance occurred due to many aspects. However, the most dominant aspects was the increased hydrodynamic pressure value. Furthermore, reducing the chord size (increasing the aspect ratio (AR) value) in each Hull Vane[®] variation had a positive impact on each speed. The most optimal Hull Vane[®] lift force value on the test ship was found in the third variation (AR = 28.94) with a value of 54,617.5 N at a speed of 11 knots.

REFERENCES

- Ghidoni, T., 2017. *Multi-Fidelity Optimization of Leading Edge Surfaces for Supersonic Drag Reduction and High-Lift Configuration*. Master Thesis. Politecnico di Milano, Milan.
- Campana, E. F., Diez, M., Liuzzi, G., Lucidi, S., Pellegrini, R., Piccialli, V., Rinaldi, F., & Serani, A., 2018. A Multi-Objective DIRECT Algorithm for Ship Hull Optimization. *Computational Optimization and Applications*, 71(1), pp. 53-72.
- Ferré, H., Goubalt, P., Yvin, C., & Bouckaert, B., 2019. Improving the Nautical Performance of a Surface Ship with the Hull Vane[®] Appendage. *The International Conference on Advanced Trends in Mechanical & Aerospace Engineering (ATMA-2019)*, Bangalore, November 7-9, pp. 1-12.
- Hall, N., 2022a. *What Is Lift?*. Available at: <https://www1.grc.nasa.gov/beginners-guide-to-aeronautics/what-is-lift/>. Accessed 2023 May 13.
- Hall, N., 2022b. *Equal Transit Theory Interactive*. Available at: <https://www1.grc.nasa.gov/beginners-guide-to-aeronautics/foilw1/>. Accessed 2023 May 13.
- Hall, N., 2022c. *Fluid Dynamics Interactive*. Available at: <https://www1.grc.nasa.gov/beginners-guide-to-aeronautics/foilinc/>. Accessed 2023 May 13.
- Riyadi, S., & Suastika, K. 2020. "Experimental and Numerical Study of High Froude-Number Resistance of Ship Utilizing a Hull Vane[®]: A Case Study of a Hard-Chine Crew Boat." *CFD Letters* Vol. 12 (2): 95-105.
- Selvaraj, R. M., Paul, P. E. S., Kumar, G. U., & Ramesh, M., 2017. Optimisation of Swept Angles for Airfoil NACA 6-Series. *International Journal of Computer Aided Engineering and Technology*, 9(2), pp. 229-240.
- Suastika, K., Saputra, A. S., & Firdhaus, A., 2020. Effectiveness of Straight and V-Shaped Vanes as Energy Saving Device Applied to High-Speed Boats. *The 12th International Conference on Marine Technology (MARTEC 2020)*, Ambon, October 15-16.
- Uithof, K., Van Oossanen, P., Moerke, N., Van Oossanen, P. G., & Zaaïjier, K. S., 2014. An Update on the Development of the Hull Vane[®]. *The 9th International Conference on High-Performance Marine Vehicles (HIPER 2014)*, Athens, December 3-5, pp. 1-11.
- White, F. M., 2011. *Fluid Mechanics 7th Edition*. New York: McGraw-Hill.

BLANK PAGE